EPJ Web of Conferences **340**, 12003 (2025) https://doi.org/10.1051/epjconf/202534012003
Powders & Grains 2025

Collective behavior of macroscopic photoactive particles: an experimental study

Sára Lévay[1,*], *Axel* Katona[1], *Hartmut* Löwen[2], *Raúl* Cruz Hidalgo[1], and *Iker* Zuriguel[1]

[1]Departamento de Física y Matemática Aplicada, Facultad de Ciencias, Universidad de Navarra, E-31080 Pamplona, Spain
[2]Institut für Theoretische Physik II: Weiche Materie, Heinrich-Heine-Universität Düsseldorf, D-40225 Düsseldorf, Germany

Abstract. We experimentally investigate the collective behavior of an active granular system in which the activity of the macroscopic self-propelled agents is controlled by light intensity. This allows us to test the system response to the agents excitation by simply changing the illumination intensity. We explore a broad range of excitation levels and population sizes, discovering the existence of a transition from stable cluster development at low excitation intensities and large population sizes to unstable clustering when the light intensity is high and the population is small. Through an extensive analysis of cluster dynamics, we have constructed a phase diagram that illustrates this transition, providing insights into the mechanisms governing collective behavior in active granular matter.

1 Introduction

Active matter systems consist of many interacting self-propelled agents that harvest energy from their environment and convert it into mechanical motion. Over the past decades, these systems have gathered significant interest across disciplines, including physics, chemistry, biology, medicine, and robotics. Examples range from microrobots [1, 2] and colloidal particles [3–5] to bacterial colonies [6], vibrated granular media [7, 8], robotic swarms [9], animal groups [10], and pedestrian dynamics [11]. Despite the differences among these systems in the interaction mechanisms, they may exhibit similarities in their emergent collective behavior, hence inspiring the development of several theoretical models to describe these phenomena [12].

The movement of active particles is often governed by a stimulus-driven response known as taxis. Depending on the nature of the stimulus, this behavior can be classified as chemotaxis, thermotaxis, viscotaxis, or magnetotaxis [13–16]. When induced by light, the phenomenon is referred to as phototaxis or photoactive behavior [1–3, 5, 6]. This study focuses on the photoactive behavior of macroscopic particles [17] on the centimeter scale. Such a system of photoactive granular matter is especially interesting as the interaction between agents occurs solely through physical contact. This facilitates the control and reproduction of experimental conditions, which is often not the case in systems, where social or hydrodynamic interactions are involved [1, 11, 12]. Furthermore, as the light source in our experiment is a fully programmable LED panel, we have complete control over the activity of the agents both in space and time. While this approach is widely applied to microscopic particles [5, 6], its application to macroscopic systems remains largely unexplored, with prior studies primarily focusing on phototactic wheeled robots [18–20]. The precise control of experimental conditions and particle activity allows our system to serve as a limit case for more sophisticated, microscopic active matter systems.

Active particles exhibiting persistent directed motion tend to accumulate at confining boundaries, leading to cluster formation [21]. The properties of these clusters – such as size distribution, stability, and internal structure – are influenced by factors including particle geometry, propulsion mechanisms, external forces, and interparticle interactions [22–24]. In this study, we focus on the clustering behavior of photoactive particles under homogeneous illumination, investigating the effect of particle activity and density on cluster formation and stability.

2 Experimental setup

The self-propelled, photosensitive agents (see Fig. 1) are adapted from Hexbug Nano particles. Each particle features ten asymmetric soft rubber legs and a vibrating motor, resulting in a propelling velocity that depends on the vibration frequency. These particles have been utilized in studies related to clogging, sorting, traffic jams, robotic superstructures, and resetting [25–29]. In this study, the battery was replaced with a 3D-printed cap holding a photovoltaic cell. This is what makes the particles photoactive: they only move when illuminated. Increased illumination intensity enhances vibration frequency, resulting in higher propulsion velocities.

The illumination is applied with a panel of LED lines mounted on an aluminum plate, covering an area of 80×80 cm^2. The LED lines are controlled by ESP32

*e-mail: slevay@unav.es

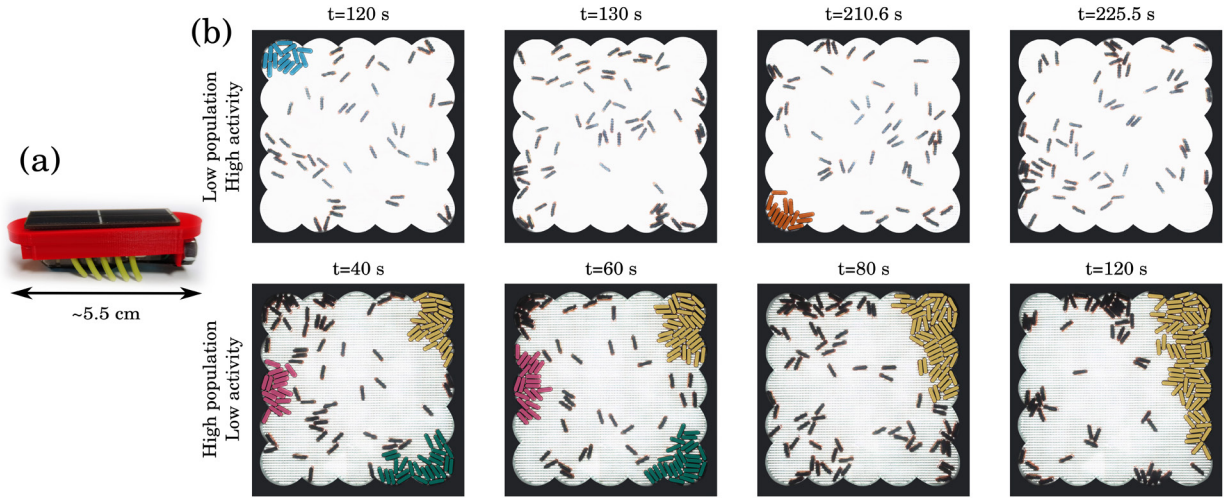

Figure 1. (a): Picture of the photoactive bug with the 3D-printed plastic cap holding the photovoltaic cell. (b): Snapshots of experiments showing the dynamics of the system. Different colors are used to identify clusters. In the first row, we present a case with a low population (N_T=60) and high activity (P=72 mW), after t=120, 130, 210.6, and 225.5 s since the beginning of the experiment. In the second row, we show a case with a high population (N_T=120) and the lowest activity level (P=23 mW) at t=40, 60, 80, and 120 s. At high activity levels, smaller clusters are formed (blue, orange) that disappear after a short time (10−15 s), while at low activity levels, larger clusters are formed with a longer lifetime. Sometimes these clusters get destroyed due to the activity of the particles inside the cluster (pink and green). Others (yellow) grow constantly and stay stable during the whole experiment, incorporating the majority of the agents.

microcontrollers, enabling precise spatiotemporal modulation of illumination fields, which regulate particle velocities between 8 to 14 cm/s. The particles move within a glass-bottomed arena enclosed by 3D-printed plastic walls (Fig. 1) that form a flower shape with the idea that particles colliding with it are redirected back to the center of the arena. A second glass plate is placed above the arena at a height slightly higher than the hexbugs, hence avoiding their tumbling in strong collisions. A camera positioned beneath the setup records particle trajectories. For more details about the experimental setup and the effect of the confining geometry on cluster dynamics, we refer the reader to [30].

In this study, we investigate the clustering behavior of photoactive particles under homogeneous illumination. We systematically vary the illumination intensity across seven levels, thereby modulating particle activity, quantified by the power (P) available for movement. Additionally, we examine five different population sizes (N_T=40, 60, 80, 100, 120). For each combination of activity level and population size, we perform five independent experiments, each lasting 6 minutes. Before each experiment, the particles were evenly distributed in rows between the two halves of the arena, facing the center. To eliminate transient effects from initial conditions, the first two minutes of each experiment are excluded from the analysis.

3 Results

As soon as the light is switched on, the particles start moving with a persistent directed motion at velocities determined by the applied intensity. When they reach a wall, if they collide with other particles moving in opposite directions, they can get trapped and start forming groups (clusters) and accumulate. In order to simplify the analysis, we consider that a group of hexbugs is a cluster when at least 4 particles are in contact for at least 1 s. Then, we track clusters throughout the experiments, measuring their duration (t_d), size (N), and maximum size ($N_{\max}$). Our results indicate that low particle activities and high population sizes promote the formation of larger, more stable clusters. This can be observed in Fig. 1 (b), where we exemplify the dynamics in two different scenarios. In the top row, we show snapshots from an experiment with high activity and low density. Even if some clusters are formed, they are small and just transient, typically dissolving within 10-15 s (blue and orange clusters). Conversely, when particle activity is low and the density is high (bottom row), larger and more stable clusters form. They can grow, merge, split, and occasionally be destroyed completely (pink and green clusters). In some cases, they become totally stable, meaning that once they are formed, they are not destroyed during the experimental time (yellow cluster). In some cases, they incorporate up to 80% of the hexbugs in the arena.

To characterize the transition from unstable to stable clustering, we analyze the cluster statistics, specifically the cluster duration (t_d) and maximum cluster size ($N_{\max}$). Both quantities exhibit power-law-like behavior, as illustrated in Fig. 2 (a-b). Here, instead of probability distribution functions, we present survival functions, which quantify the probability of finding clusters with a duration or size exceeding a given threshold. Fig. 2 (a) displays the cluster duration survival function for three different cases: two population sizes (N_T=80 and 120) at the lowest particle activity level (P=23 mW) (shown in light and dark green, respectively), and N_T=80 at the high-

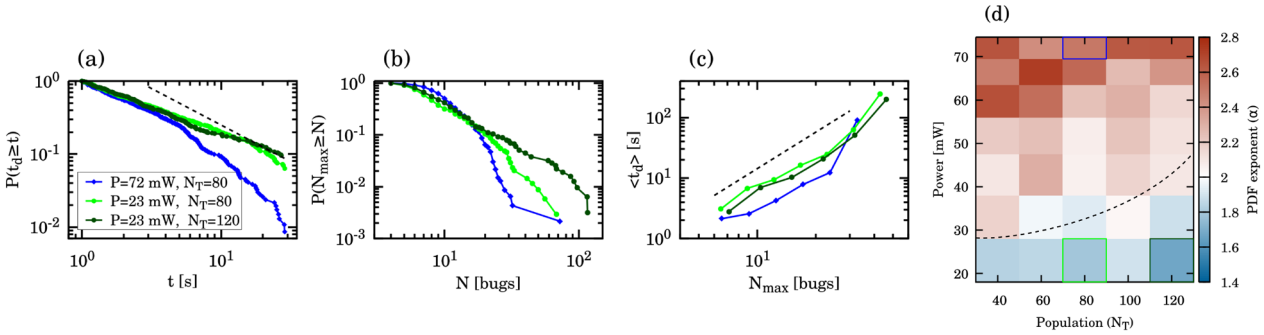

Figure 2. (a): Cluster duration survival functions, $P(t_d \geq t)$, for three populations and illumination levels. The dashed line represents a power law with exponent 1, which means an exponent for the PDF: α=2. (b): Maximum cluster size survival function for the same populations and illuminations as in panel (a). (c): The average duration of clusters vs. the maximum cluster size for the same populations and activities as in panel (a). The dashed line shows a power law with exponent 2. (d): Phase diagram of the cluster stability, based on the fitted α exponents of the cluster duration PDFs for all the population and illumination levels. Red colors show α>2, while blue colors correspond to α<2 values. The latter marks the presence of stable clusters, while the former corresponds to unstable clusters in the system. Values close to 2 (white and light region) mark the transition between the two phases, which is also visualized by the dashed line. The colored solid rectangles show the three cases presented in panels (a-c).

est activity level (P=72 mW) (shown in blue). Clearly, for such low activity level, increasing the population size has a minimal effect on the survival function (comparison between the green curves). However, increasing activity (while keeping the population size constant) significantly reduces cluster duration (comparison between the light green and blue curves). Similarly, Fig. 2 (b) presents the survival function of the maximum cluster size, where the three cases exhibit clear separation. Larger populations and lower activity levels result in larger clusters. Notably, we see a clear relation between the cluster duration and the maximum cluster size. This relationship is explicitly demonstrated in Fig. 2 (c), which shows that larger clusters tend to persist for longer durations.

To quantify further the transition from unstable to stable clustering, we obtained the cluster stability phase diagram (Fig. 2 (d)) by fitting the tail of the cluster duration probability distribution function (PDF) for all population and activity levels. (Note that a power-law PDF with an exponent α corresponds to a survival function with exponent $\alpha - 1$.) The system can be classified into two distinct regimes. Red regions (α>2) correspond to high activity and low populations, while blue areas (α<2) are associated with low activity and high population. Notably, when α<2, the average cluster duration diverges, strongly correlating with the presence of stable clusters in the system.

Lastly, aiming to get an insight into the cluster dynamics, we analyzed their time evolution. In the experiments, we observe that cluster growth occurs mostly by the attachment of individual particles. However, sometimes, smaller groups of particles can collide and merge into a large cluster. On the other hand, apart from individual particles departing from a cluster, cluster dissolution shows bursts of particles leaving the cluster with avalanche-like dynamics. Smaller subgroups tend to move together and split from the group. Inspired by [4], we have calculated the transition matrices for experiments with high populations (N_T=100 and 120), for low (P=23 and 33 mW) and high intensities (P=67 and 72 mW). The transition matrices (Fig. 3 (a)) show the probability $P(N_1|N_0, \Delta t)$ for a cluster of size N_0 to have a size of N_1 after a time lag Δt. We used two different time lags in the calculations, Δt=1τ and 10τ, where τ is the characteristic time a bug needs to move a distance of its length at an intermediate activity level. As expected, for small Δt (top panels), we observe values close to 1 in the N_0=N_1 line, with small but nonzero elements around it. This means that in this short time, a cluster most probably stays the same, or its change is due to individual particles attaching to or detaching from the cluster. This is also visible in panel (b), where we show the transition probabilities for N_0=40 and 60 (marked with blue and red in panel (a)). However, if we take the larger time lag, Δt=10τ, the symmetry around the N_0=N_1 line changes. Nonzero elements are more spread, and the transition probabilities are higher below the N_0=N_1 line, a result supported by the asymmetry of transition probabilities reported in panels of Fig. 3 (c). Altogether, these results indicate that the probability of having small groups of particles leaving the cluster together is much higher than the probability that a small cluster attaches to a big one.

4 Discussion & Outlook

In this study, we investigate the collective behavior, specifically the cluster dynamics, using a novel class of photoactive macroscopic particles. We identify a stable clustering phase at low particle activity and high population sizes, whereas, at high activity and low population sizes, clusters dissolve rapidly and are thus unstable. We study the time evolution of clusters through transition probabilities, which suggests that although the cluster growth can be seen as individual particles attaching to clusters, the dissolution of clusters involves the collective detachment of small subgroups of particles.

The versatility of the presented experimental setup, namely the fully programmable external control on the

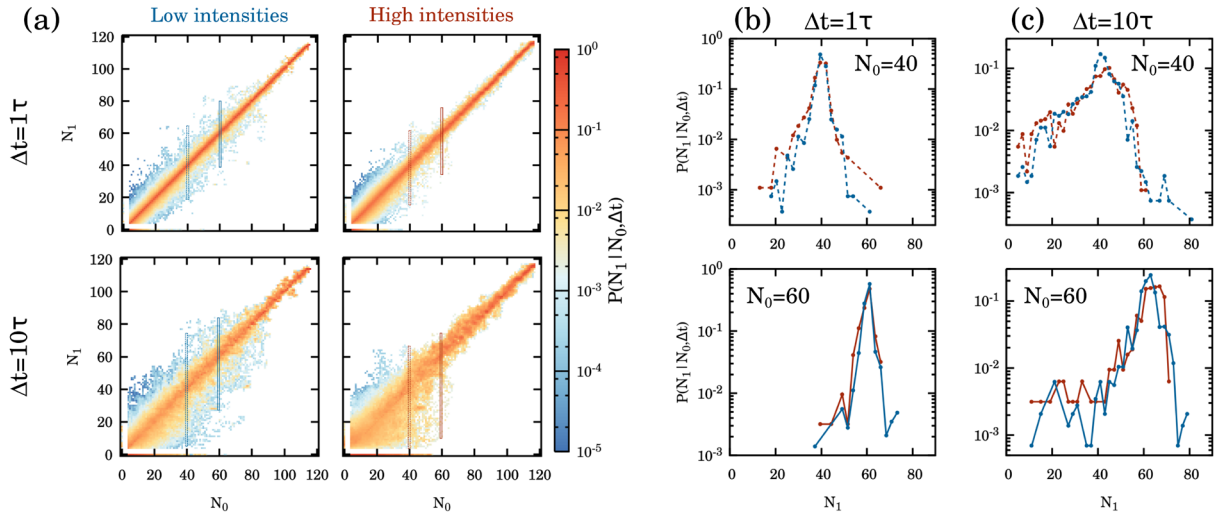

Figure 3. (a): Transition matrices showing the probability $P(N_1|N_0, \Delta t)$ for a cluster of size N_0 to have a size of N_1 after a time lag Δt. The matrices are calculated for experiments with populations of N=100 and 120, for low intensities (P=23 and 33 mW) and high intensities (P=67 and 72 mW), and for Δt=1τ and 10τ, where τ is the characteristic time a bug needs to move a distance of its length at an intermediate activity level. (The sampling time of the experiment was 0.067τ.) (b): Transition probabilities for N_0=40 (dashed) and 60 (continuous), and for low (blue) and high (red) intensities, for the two different time lags.

particle activity through illumination, enables us to study more complex scenarios of collective behavior, with spatiotemporally varying activity fields. The results of collective behavior under homogeneous illuminations presented here help us to understand the response of the system in ongoing studies, e.g., in the case of alternating activity levels or wave-like activity patterns in the system.

Acknowledgements

We thank Luis Fernando Urrea and Lucia Sastre for technical help. This project has been funded by the European Union's Horizon 2020 research and innovation program under the Marie Skłodowska-Curie grant agreement No. 101067363 named PhotoActive and the Spanish Government, through grant No. PID2023-146422NB-I00 supported by MICIU/AEI/10.13039/501100011033. A. K. acknowledges the Asociación de Amigos, Universidad de Navarra, for his grant.

References

[1] S. Palagi et al., Nat. Mater. **15**, 647 (2016).
[2] M.Z. Miskin et al., Nature **584**, 557 (2020).
[3] C. Lozano et al., Nat. Commun. **7**, 12828 (2016).
[4] F. Ginot et al., Nat. Commun. **9**, 696 (2018).
[5] H.R. Vutukuri et al., Nat. Commun. **11**, 2628 (2020).
[6] J. Arlt et al., Nat. Commun. **9**, 768 (2018).
[7] C. Scholz et al., Nat. Commun. **9**, 931 (2018).
[8] M. Mohammadi et al., New J. Phys. **22**, 123025 (2020).
[9] H. Oh et al., Rob. Auton. Syst. **91**, 83 (2017).
[10] F. Ginelli et al., PNAS **112**, 12729 (2015).
[11] A. Corbetta et al., Annu. Rev. Condens. Matter Phys. **14**, 311 (2023).
[12] T. Vicsek et al., Phys. Rep. **517**, 71 (2012).
[13] B. Liebchen et al., Acc. Chem. Res. **51**, 2982 (2018).
[14] I. Mori et al., Nature **376**, 344 (1995).
[15] B. Liebchen et al., Phys. Rev. Lett. **120**, 208002 (2018).
[16] M. Sun et al., Nanoscale **11**, 18382 (2019).
[17] F. Siebers et al., Sci. Adv. **9**, eadf5443 (2023).
[18] M. Mijalkov et al., Phys. Rev. X **6**, 011008 (2016).
[19] M. Leyman et al., arXiv preprint arXiv:1807.11765 (2018).
[20] M. Rey et al., ACS Photonics **10**, 1188 (2023).
[21] N.A.M. Araújo et al., Soft Matter **19**, 1695 (2023).
[22] S. Thapa et al., New J. Phys. **26**, 023010 (2024).
[23] M. Becton et al., Nanomaterials **14**, 144 (2024).
[24] L. Caprini et al., Commun. Phys. **7**, 343 (2024).
[25] G.A. Patterson et al., Phys. Rev. Lett. **119**, 248301 (2017).
[26] T. Barois et al., Phys. Rev. E **99**, 052605 (2019).
[27] J.F. Boudet et al., Sci. Robot. **6**, eabd0272 (2021).
[28] P. Baconnier et al., Nat. Phys. **18**, 1234 (2022).
[29] A. Altshuler et al., Phys. Rev. Res. **6**, 023255 (2024).
[30] S. Lévay et al., arXiv preprint arXiv:2412.14419 (2024).